

Stochastic Quantum Information Geometry and Speed Limits at the Trajectory Level

Pedro B. Melo,^{1,2,*} Pedro V. Paraguassú,² Sílvio M. Duarte Queirós,³ Fernando Iemini,⁴ Mauro Paternostro,^{1,5} and Welles A. M. Morgado²

¹Università degli Studi di Palermo, Dipartimento di Fisica e Chimica - Emilio Segrè, via Archirafi 36, I-90123 Palermo, Italy

²Departamento de Física, PUC-Rio, 22452-970, Rio de Janeiro RJ, Brazil

³Centro Brasileiro de Pesquisas Físicas, 22452-970, Rio de Janeiro RJ, Brazil

⁴Departamento de Física, Universidade Federal Fluminense, 22452-970, Niterói RJ, Brazil

⁵Centre for Quantum Materials and Technologies, School of Mathematics and Physics,
Queen's University Belfast, BT7 1NN, United Kingdom

(Dated: January 21, 2026)

Standard quantum metrology relies on ensemble-averaged quantities, such as the Quantum Fisher Information (QFI), which often mask the fluctuations inherent to single-shot realizations. In this work, we bridge the gap between quantum information geometry and stochastic thermodynamics by introducing the Conditional Quantum Fisher Information (CQFI). Defined via the Symmetric Logarithmic Derivative, the CQFI generalizes the classical stochastic Fisher information to the quantum domain. We demonstrate that the CQFI admits a decomposition into incoherent (population) and coherent (basis rotation) contributions, augmented by a transient interference cross-term absent at the ensemble level. Crucially, we show that this cross-term can be negative, signaling destructive interference between classical and quantum information channels along individual trajectories. Leveraging this framework, we construct a stochastic information geometry that defines thermodynamic length and action for single quantum trajectories. Finally, we derive fundamental quantum speed limits valid at the single-trajectory level and validate our results using the quantum jump unraveling of a driven thermal qubit.

I. INTRODUCTION

The Quantum Fisher Information (QFI) stands as a cornerstone of quantum metrology, quantifying the ultimate sensitivity of a quantum system to changes in an underlying parameter. By establishing the quantum Cramér-Rao bound, the QFI dictates the fundamental precision limits for parameter estimation, constrained only by the laws of quantum mechanics [1–4]. This framework has proven indispensable across diverse physical systems, from single-qubit sensors [5, 6] to complex many-body quantum simulators [7, 8].

Traditionally, the QFI is employed to assess precision based on ensemble-averaged probability distributions obtained from repeated measurements. This ensemble approach underpins key protocols such as quantum state tomography [9] and optical phase estimation in noisy interferometry [10, 11]. More recently, the QFI has found profound utility in the study of quantum critical phenomena, where its divergence near critical points signals that criticality can be harnessed to dramatically enhance metrological precision, a resource known as critical metrology [12–14]. Furthermore, the QFI has provided a rigorous geometric basis for deriving quantum speed limits (QSLs) in open systems, bounding the rate of evolution for non-unitary processes subject to environmental decoherence [15–17].

Parallel developments in classical stochastic thermodynamics have established the Fisher Information

(FI) as a fundamental metric for thermodynamic state spaces. Beyond its metrological origins, the FI has emerged as a geometric measure connecting information theory to thermodynamics, particularly for near-equilibrium states [18–20]. The thermodynamic length and action, derived from the FI metric, have been shown to relate directly to excess work and dissipation in driven systems. These results have been generalized to arbitrarily far-from-equilibrium systems [21, 22], enabling the derivation of fundamental speed limits for the evolution of both states and observables in classical stochastic processes [23–25].

Recent advances have begun to bridge the gap between information geometry and the fluctuating energetics of small quantum systems. In the classical domain, the Stochastic Fisher Information (SFI) has been introduced to quantify the "surprise" rate of individual trajectories and establish speed limits for state transformations at the level of single realizations [26]. This trajectory-level perspective has proven particularly valuable for understanding rare events and non-typical fluctuations that are masked in ensemble averages [27, 28]. However, a fully quantum generalization that accounts for the intricate interplay between classical population statistics and quantum coherence evolution along individual measurement trajectories has remained an open challenge.

The difficulty in extending stochastic information geometry to the quantum domain stems from several fundamental aspects. First, quantum measurements inevitably disturb the system state, leading to trajectory-dependent evolution that differs qualitatively from classical stochastic processes [29, 30]. Second, the

* pedrobmelo@aluno.puc-rio.br

quantum superposition principle introduces correlations between population dynamics and coherent evolution that have no classical analog. Finally, the choice of measurement basis fundamentally affects the observed trajectory statistics, requiring a framework that can account for arbitrary measurement schemes while preserving the connection to fundamental quantum limits.

In this work, we address these challenges by introducing the Conditional Quantum Fisher Information (CQFI), which generalizes the classical SFI to the quantum domain while preserving its trajectory-level interpretation. Defined via the Symmetric Logarithmic Derivative (SLD) and conditioned on specific measurement outcomes, the CQFI extends quantum metrology from ensemble averages to single-shot realizations. Unlike the standard QFI, which provides a global bound averaged over all possible measurement outcomes, the CQFI is a random variable that fluctuates along individual quantum trajectories.

Our approach yields several contributions of relevance for quantum metrology and stochastic thermodynamics. First, we demonstrate that the CQFI admits a physically transparent decomposition into three distinct contributions: (i) an *incoherent* term arising from population changes, analogous to the classical SFI; (ii) a *coherent* term arising from unitary rotations of the eigenbasis; and (iii) a *cross-term* representing interference between classical and quantum channels. We show that the latter term can be negative, signifying destructive interference between the evolutions of population and coherences along individual trajectories, which is a purely quantum phenomenon that disappears at ensemble level. Figure 1 depicts this interference effect in a sketch, showing that on trajectory level negative contributions to the CQFI can appear, while on ensemble average they are zero.

Second, leveraging this decomposition, we construct a stochastic information geometry that defines thermodynamic length and action for individual quantum trajectories. This geometric framework allows us to quantify the statistical distance traversed by a quantum system in a single experimental realization, extending the tools of information geometry from ensemble descriptions to the realm of individual quantum measurements.

Third, we derive fundamental quantum speed limits valid at the single-trajectory level, generalizing both classical stochastic bounds [26] and ensemble quantum speed limits [15, 16] to the intersection of these domains. We demonstrate that such trajectory-level bounds can be significantly tighter than their ensemble counterparts, particularly in regimes dominated by unlikely-to-occur but informative quantum trajectories.

Finally, we validate our theoretical framework through detailed numerical simulations using two paradigmatic systems: the quantum jump unraveling of a driven thermal qubit and the continuous monitoring of displaced

Gaussian states. These examples demonstrate that our trajectory-level bounds provide useful insights into quantum information dynamics that are not accessible through ensemble-averaged approaches.

The remainder of this paper is organized as follows. Sec. II introduces the CQFI formalism and derives its spectral decomposition into incoherent, coherent, and interference contributions. Sec. III applies the CQFI framework to construct a stochastic information geometry with time as the estimation parameter. Section IV derives trajectory-level quantum speed limits and presents comprehensive numerical validations using quantum jump trajectories. In Sec. V we draw our conclusions, which include a discussion of applications in adaptive quantum metrology, real-time quantum feedback, and single-trajectory thermodynamic protocols. A set of appendices report the technical aspects of our derivations.

II. CONDITIONAL QUANTUM FISHER INFORMATION

Consider a physical system described by a probability distribution $p(x|\theta)$, where x represents an accessible physical parameter of the system (such as position, momentum, or a measurement outcome) and θ is an unknown parameter to be estimated.

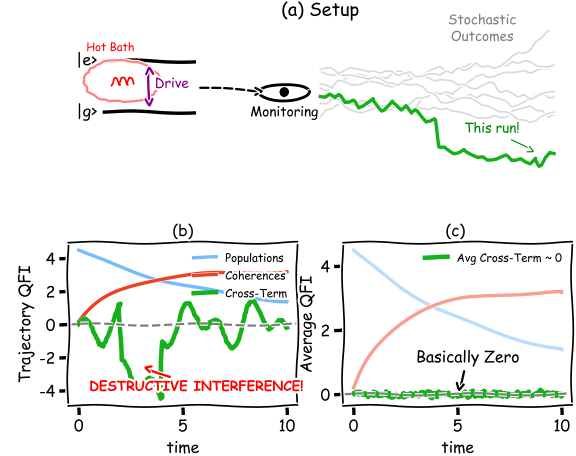


FIG. 1. Sketch of the conditional quantum Fisher information for the adopted example in this work. Panel (a) shows a sketch of a qubit in contact with a thermal bath, submitted to a driving potential. When the system is monitored, it produces stochastic outcomes for each realization. Panel (b) depicts the results for trajectory level quantum Fisher information decomposed into the contributions from population changes in blue, the contributions from unitary rotations of the eigenbasis in red, and the cross contributions from the interference between both channels in green. Panel (c) shows the results from the averaged QFI on ensemble level, where the cross contributions vanish.

The classical Fisher information (FI) for θ is defined as the expectation value of the squared score function (the derivative of the log-likelihood)

$$\mathcal{F}(\theta) = \sum_x p(x|\theta) \left(\frac{\partial \log p(x|\theta)}{\partial \theta} \right)^2. \quad (1)$$

An analogous quantity is the Stochastic Fisher information (SFI), recently introduced in the context of stochastic thermodynamics [26, 31]. The SFI is a random variable whose average yields the FI. Unlike the standard FI, the SFI $\iota(x, \theta)$ depends on the specific single-shot realization x

$$\iota(x, \theta) = \left(\frac{\partial \log p(x|\theta)}{\partial \theta} \right)^2. \quad (2)$$

The SFI effectively quantifies the “surprisal” rate with respect to the parameter θ . The stochastic thermodynamic interpretation of the SFI closely mirrors that of the FI, maintaining the analogy between fluctuating (trajectory-level) and averaged quantities. Furthermore, the SFI provides speed limits for state transformations at the single-trajectory level [26].

A. Quantum Fisher information

The quantum Fisher information (QFI) generalizes the FI to quantum systems [1]. We define the conditional probability distribution via the Born rule as $p(x|\theta) = \text{Tr}(\Pi_x \rho_\theta)$, where $\Pi_x = |x\rangle\langle x|$ is a projector onto the state $|x\rangle$, and ρ_θ is a quantum state in a Hilbert space \mathcal{H} parameterized by $\theta \in \mathcal{M}$ (a d -dimensional manifold). This definition generalizes to cases where $\{\Pi_x\}$ forms an arbitrary positive operator-valued measure (POVM).

In contrast to the classical setting, the Chentsov-Petz theorem establishes that the choice of Fisher metric for density matrices is not unique [32]. Using the spectral decomposition $\rho_\theta = \sum_x p_x(\theta) |x(\theta)\rangle\langle x(\theta)|$, the general QFI is given by

$$\mathcal{F}_Q(\theta) = \sum_{x,y} \frac{|\langle x(\theta) | \partial_\theta \rho_\theta | y(\theta) \rangle|^2}{p_x(\theta) f(p_y(\theta)/p_x(\theta))}, \quad (3)$$

where f is an operator monotone function (self-inverse $f(t) = tf(1/t)$ and normalized $f(1) = 1$). We focus on the Symmetric Logarithmic Derivative (SLD) QFI, corresponding to $f_{\text{SLD}}(t) = (t+1)/2$. In this case, $\mathcal{F}_Q(\theta)$ simplifies to

$$\mathcal{F}_Q(\theta) = 2 \sum_{x,y} \frac{|\langle x(\theta) | \partial_\theta \rho_\theta | y(\theta) \rangle|^2}{p_x(\theta) + p_y(\theta)}, \quad (4)$$

where the sum runs over indices with $p_x + p_y > 0$. Unless otherwise stated, we refer to the SLD-based quantity simply as the QFI.

We introduce the SLD operator L_θ , implicitly defined by the Lyapunov equation

$$\frac{\partial \rho_\theta}{\partial \theta} = \frac{1}{2} \{L_\theta, \rho_\theta\}, \quad (5)$$

where $\{\cdot, \cdot\}$ denotes the anti-commutator. In the spectral basis of ρ_θ , L_θ takes the form

$$L_\theta = \sum_x \frac{\partial_\theta p_x(\theta)}{p_x(\theta)} |x(\theta)\rangle\langle x(\theta)| + 2 \sum_{x \neq y} \left(\frac{p_x(\theta) - p_y(\theta)}{p_x(\theta) + p_y(\theta)} \right) \langle x(\theta) | \partial_\theta y(\theta) \rangle |x(\theta)\rangle\langle y(\theta)|. \quad (6)$$

The QFI is then given by the second moment of the SLD operator $\mathcal{F}_Q(\theta) = \text{Tr}(\rho_\theta L_\theta^2)$. Replacing Eq. (6) in the trace, we obtain the decomposition $\mathcal{F}_Q(\theta) = \mathcal{F}_Q^{\text{IC}}(\theta) + \mathcal{F}_Q^{\text{C}}(\theta)$ with

$$\mathcal{F}_Q^{\text{IC}}(\theta) = \sum_x \frac{(\partial_\theta p_x(\theta))^2}{p_x(\theta)}, \quad (7)$$

$$\mathcal{F}_Q^{\text{C}}(\theta) = 2 \sum_{x \neq y} \sigma_{xy} |\langle y(\theta) | \partial_\theta x(\theta) \rangle|^2,$$

where we have introduced the coefficients $\sigma_{xy} = \frac{(p_x(\theta) - p_y(\theta))^2}{p_x(\theta) + p_y(\theta)}$ [1]. This decomposition identifies an incoherent contribution to the QFI, associated with $\mathcal{F}_Q^{\text{IC}}(\theta)$ and stemming from a change in the populations, and a coherent one encompassed by $\mathcal{F}_Q^{\text{C}}(\theta)$, which arises from the rotation of the eigenvectors with respect to the instantaneous basis.

B. Conditional Quantum Fisher Information

We now introduce the quantum generalization of the SFI, which we dub *Conditional Quantum Fisher Information* (CQFI). Recall that the SFI describes the information content of a single measurement outcome purely from the trajectory statistics. In the quantum regime, we must account for how the global state structure dictates local sensitivity.

Let $\{\Pi_\alpha\}$ be a general POVM, where α labels the measurement outcome. The conditional probability is $p(\alpha|\theta) = \text{Tr}(\Pi_\alpha \rho_\theta)$. From Eq. (2), the SFI associated with outcome α is

$$\iota(\alpha, \theta) = \left(\frac{\partial \log p(\alpha|\theta)}{\partial \theta} \right)^2 = \left(\frac{\text{Tr}(\Pi_\alpha \partial_\theta \rho_\theta)}{\text{Tr}(\Pi_\alpha \rho_\theta)} \right)^2. \quad (8)$$

Using the Cauchy-Schwarz and trace identities (see Appendix A), we define the CQFI for a specific outcome α as

$$f_{Q,\alpha}(\theta) = \frac{\text{Tr}(\Pi_\alpha L_\theta^2 \rho_\theta)}{\text{Tr}(\Pi_\alpha \rho_\theta)}. \quad (9)$$

Physically, the CQFI represents the QFI conditioned on a specific POVM element. It quantifies the local power of the SLD generator sampled by the outcome α . Note that while $f_{Q,\alpha}(\theta)$ is a random variable associated with a single realization, it relies on the operator L_θ , which is defined globally via the ensemble density matrix ρ_θ .

The CQFI naturally averages to the total QFI over the measurement statistics. Using the completeness relation $\sum_\alpha \Pi_\alpha = \mathbb{I}$, we have

$$\begin{aligned} \langle f_{Q,\alpha}(\theta) \rangle_{\{\Pi_\alpha\}} &= \sum_\alpha p(\alpha|\theta) f_{Q,\alpha}(\theta) \\ &= \text{Tr} \left[\left(\sum_\alpha \Pi_\alpha \right) L_\theta^2 \rho_\theta \right] = \mathcal{F}_Q(\theta). \end{aligned} \quad (10)$$

Alternatively, an equivalent representation of the CQFI is given by $f_{Q,\alpha}(\theta) = \text{Tr}(\Pi_\alpha L_\theta^2)$. A key advantage of the CQFI is that it allows for the clear identification of contributions stemming from the interplay between classical statistics and quantum coherence. Assuming $\Pi_\alpha = |\alpha\rangle\langle\alpha|$, the CQFI can be written as (cf. Appendix B)

$$f_{Q,\alpha}(\theta) = f_{Q,\alpha}^{IC}(\theta) + f_{Q,\alpha}^C(\theta) + f_{Q,\alpha}^X(\theta). \quad (11)$$

The first two terms are the incoherent and coherent contribution, respectively, analogous to the ensemble-based expression

$$f_{Q,\alpha}^{IC}(\theta) = \sum_n \left(\frac{\partial_\theta p_n}{p_n} \right)^2 |\langle n|\alpha\rangle|^2, \quad (12)$$

$$f_{Q,\alpha}^C(\theta) = \sum_k \left| \sum_{n(\neq k)} \langle n|\alpha\rangle \frac{2(p_n - p_k)}{p_n + p_k} \langle k|\partial_\theta n\rangle \right|^2. \quad (13)$$

Crucially, at the single-outcome level, the cross-term $f_{Q,\alpha}^X$ appears in Eq. (11). Explicitly, we have that

$$\begin{aligned} f_{Q,\alpha}^X(\theta) &= \sum_{k \neq n} \text{Re} \left[\langle \alpha|k(\theta)\rangle \langle n(\theta)|\alpha\rangle \left(\frac{\partial_\theta p_k}{p_k} + \frac{\partial_\theta p_n}{p_n} \right) \right. \\ &\quad \left. \times \left(\frac{2(p_n - p_k)}{p_n + p_k} \right) \langle k|\partial_\theta n\rangle \right], \end{aligned} \quad (14)$$

thus showing that such genuinely trajectory-dependent contribution arises from the interference between population shifts and basis rotations. Unlike the incoherent and coherent terms, which are strictly non-negative, the cross-term f_Q^X can be negative. While, at first sight, this might appear counterintuitive, negative values imply destructive interference, where the classical re-weighting of probabilities and the quantum rotation of the basis act in opposition relative to the probe state $|\alpha\rangle$. This interference effect is a strictly local feature: when averaged over the ensemble, the cross-term vanishes ($\langle f_Q^X \rangle = 0$), allowing us to recover the standard decomposition of the QFI. If the measurement basis coincides with the spectral basis of ρ_θ (i.e., $|\alpha\rangle =$

$|x\rangle$), both the coherent and cross term vanish, and $f_{Q,x}(\theta)(x, \theta) = f_{Q,x}^{IC}(\theta)$, thus recovering the classical SFI limit. This is the case, for example, under quasi-static or adiabatic evolutions, where the system remains in an eigenstate.

This embodies a key central result of our study: the CQFI generalizes the SFI to the quantum domain, preserving the decomposition into probability evolution and basis rotation, while unveiling the transient interference hidden in ensemble averages. To approach the quantum thermodynamic geometry [33] conditioned to the trajectory level, in the following Section, we make use of the CQFI with respect to time as a metric.

III. CONDITIONAL QUANTUM FISHER INFORMATION WITH RESPECT TO TIME

The estimation of time is not limited to clock synchronization protocols; it also enables a rigorous connection between the CQFI, speed limits, and stochastic thermodynamics. To this end, we hereby construct the CQFI formalism with time as the estimated parameter, setting the stage for the discussion on speed limits that follows.

A. Classical framework

Let us consider a path defined by a set of discrete probability distributions $\{p_x(t)\}$ over discrete states $x \in X$, evolving over a time interval from $t = 0$ to $t = \tau$. Assuming the system is controlled by a finite set of time-dependent parameters $\theta(t) = (\theta_1(t), \dots, \theta_M(t))$, the path is confined to a statistical manifold $\Theta = \{p(x|\theta(t))\}$. Treating time t as the parameter of interest (i.e. $\theta_1(t) = \theta_2(t) = \dots = \theta_M(t) = t$), the Fisher information (FI) is given by

$$\mathcal{I}(t) = \sum_x p_x(t) \left(\frac{d \log p_x(t)}{dt} \right)^2. \quad (15)$$

The FI induces a metric structure on the manifold, given by the line element

$$ds^2 = \frac{1}{4} \mathcal{I}(t) dt^2. \quad (16)$$

This allows for the definition of the thermodynamic length

$$\mathcal{L}(t) = \frac{1}{2} \int_0^t d\tau \sqrt{\mathcal{I}(\tau)}, \quad (17)$$

which represents a distance on the statistical manifold. The derivative $ds/dt = \frac{1}{2} \sqrt{\mathcal{I}(t)}$ expresses the instantaneous statistical speed. The statistical divergence, or thermodynamic action, is defined as

$$\mathcal{J}(t) = \frac{t}{4} \int_0^t d\tau \mathcal{I}(\tau). \quad (18)$$

This quantity is analogous to a kinetic energy integral and serves as a bound to the squared statistical distance via the Cauchy-Schwarz inequality, $\mathcal{J}(t) \geq \mathcal{L}^2(t)$.

When considering single realizations of the dynamics, the stochastic Fisher information (SFI) with respect to time adopts the form [26]

$$\iota(x, t) = \left(\frac{d \log p_x(t)}{dt} \right)^2. \quad (19)$$

Given that the underlying dynamics are stochastic, $\iota(x, t)$ satisfies the requirements for a random metric on the statistical manifold. The stochastic length $\ell[x(t)]$ for a specific path (sequence of states $x(t)$) is defined as

$$\ell[x(t)] = \frac{1}{2} \int_0^t d\tau \sqrt{\iota(x, \tau)}. \quad (20)$$

Similarly, the stochastic divergence $j[x(t)]$ is given by

$$j[x(t)] = \frac{t}{4} \int_0^t d\tau \iota(x, \tau), \quad (21)$$

which bounds the squared stochastic velocity according to $j[x(t)] \geq \ell^2[x(t)]$.

B. Quantum framework

This framework generalizes to the quantum setting by considering the CQFI of Eqs.(12)–(14) with time t as the estimation parameter. Previous studies have analyzed this decomposition at the ensemble level, where the cross-terms vanish upon averaging, leaving the total QFI as the sum of an incoherent contribution $\mathcal{F}_Q^{\text{IC}} = \lim_{N_{\text{trajs}} \rightarrow \infty} \langle f_Q^{\text{IC}} \rangle$ and a coherent contribution $\mathcal{F}_Q^{\text{C}} = \lim_{N_{\text{trajs}} \rightarrow \infty} \langle f_Q^{\text{C}} \rangle$. The term \mathcal{F}_Q^{C} serves as a measure of coherence utility. Recently, Bettmann and Goold [34] utilized this ensemble decomposition to provide a thermodynamic interpretation of $\mathcal{F}_Q^{\text{IC}}$ and derived bounds on the entropic velocity using \mathcal{F}_Q^{C} .

Our work establishes a trajectory-level approach to these quantities. To do so, we employ the quantum trajectory formalism, specifically the quantum jump method (or Monte Carlo Wave Function method) [35].

We assume the system evolves under a Gorini-Kossakowski-Sudarshan-Lindblad (GKSL) master equation

$$\frac{d\rho_t}{dt} = -\frac{i}{\hbar} [H_t, \rho_t] + \mathcal{D}[\rho_t], \quad (22)$$

with the dissipator

$$\mathcal{D}[\rho_t] = \sum_k \left(L_k \rho_t L_k^\dagger - \frac{1}{2} \{ L_k^\dagger L_k, \rho_t \} \right). \quad (23)$$

Here, $\{L_k\}$ is a set of jump operators satisfying the detailed balance condition $L_{k-} = L_{k+} e^{-\Delta s_k/2}$, with

$L_{k+} = \sqrt{\Gamma_+} L_k^\dagger$, $L_{k-} = \sqrt{\Gamma_-} L_k$ and Δs_k represents the stochastic entropy flow from the system to the environment, associated to the reversible part of entropy changes due to the interaction between the system and the environment [36, 37]. While the GKSL equation describes the ensemble dynamics, we unravel this master equation into individual quantum trajectories. A single trajectory is described by a pure state $|\psi_\gamma(t)\rangle$, labeled by the realization index γ . The ensemble state is recovered via the statistical average $\rho_t = \mathbb{E}[|\psi_\gamma(t)\rangle\langle\psi_\gamma(t)|]$.

The stochastic Schrödinger equation (SSE) governing the evolution of a single trajectory is

$$\begin{aligned} d|\psi_\gamma(t)\rangle = & \left[-\frac{i}{\hbar} H_{\text{eff}}(t) + \frac{1}{2} \sum_k \|L_k|\psi_\gamma(t)\rangle\|^2 \right] |\psi_\gamma(t)\rangle dt \\ & + \sum_k \left[\frac{L_k}{\|L_k|\psi_\gamma(t)\rangle\|} - 1 \right] |\psi_\gamma(t)\rangle dN_k(t), \end{aligned} \quad (24)$$

where $H_{\text{eff}}(t) = H(t) - \frac{i\hbar}{2} \sum_k L_k^\dagger L_k$ is the non-Hermitian effective Hamiltonian. The term $dN_k(t)$ represents a Poisson process increment such that $dN_k = 1$ if a jump occurs and 0 otherwise, with ensemble average $\mathbb{E}[dN_k] = \|L_k|\psi_\gamma\rangle\|^2 dt$.

The probability of observing a specific trajectory $\gamma_{[0, \tau]} = \{n_0, \gamma_{(0, \tau)}, n_\tau\}$ is given by $P_\Lambda(\gamma_{[0, \tau]}) = p_{n_0}^0 \text{Tr}[\Pi_{n_\tau}^\tau \mathcal{T}_\Lambda(\gamma_{[0, \tau]}) \Pi_{n_0}^0 \mathcal{T}_\Lambda^\dagger(\gamma_{[0, \tau]})]$, where the trajectory is bookended by projective measurements Π_n^0 and Π_n^τ in the eigenbasis of the system.

We define the stochastic length for a single trajectory γ as

$$\ell(\gamma, t) = \frac{1}{2} \int_0^t d\tau \sqrt{f_{Q,\gamma}(\tau)}, \quad (25)$$

and the single-trajectory action as

$$j(\gamma, t) = \frac{t}{4} \int_0^t d\tau f_{Q,\gamma}(\tau). \quad (26)$$

Unlike the ensemble statistical action, which relates to a geodesic distance on the statistical manifold, the single-trajectory action $j(\gamma, t)$ does not strictly represent a divergence from a geodesic path, as geodesics are ill-defined for the stochastic metric itself. However, $j(\gamma, t)$ remains a useful quantity due to the Cauchy-Schwarz inequality $j(\gamma, t) \geq \ell^2(\gamma, t)$. Furthermore, as shown in classical stochastic thermodynamics [26], the hierarchy of speed limits holds on average $\mathcal{J}(t) \geq \mathcal{L}^2(t) \geq \text{Var}\{\ell[\gamma]\}$.

To characterize the stochastic information geometry at the trajectory level, we observe that, at each time step t , the CQFI is conditioned on the instantaneous pure state of the trajectory $|\psi_\gamma(t)\rangle$. By making the spectral decomposition of the ensemble density matrix we can determine the projection of the state at a given time for one trajectory onto each of the eigenstates of the system $\langle n(t)|\psi_\gamma(t)\rangle$.

IV. QUANTUM SPEED LIMITS ON THE TRAJECTORY LEVEL

Having introduced the formalism of quantum trajectories, we can now define stochastic dynamics to develop the quantum analogue of speed limits for single trajectories [26]. Significant progress has been made in understanding quantum speed limits (QSLs) for open system dynamics and their thermodynamic interpretation. For instance, QSLs have been derived for open systems [15, 16] and generalized to infinite families of metrics [38]. Also, thermodynamic interpretations have been given to the Fisher information [21, 22, 24] and, more recently, to the QFI [34]. Here, we extend the stochastic results of Ref. [26] to the quantum regime and the ensemble-level results of Ref. [34] to the trajectory level.

From the Cauchy-Schwarz inequality applied to the stochastic geometric quantities, $j[\rho_\gamma(t)] \geq \ell^2[\rho_\gamma(t)]$, it follows that the time-averaged variance of the CQFI is non-negative [22, 34]

$$\delta[\rho_\gamma(t)] = 4 \frac{j[\rho_\gamma(t)] - \ell^2[\rho_\gamma(t)]}{t^2} \geq 0, \quad (27)$$

where $j[\rho_\gamma(t)]$ and $\ell[\rho_\gamma(t)]$ are the accumulated action and length up to time t . Due to their stochastic nature along a single trajectory, it is impossible to define a geodesic in the same sense as the ensemble QFI geometric quantities \mathcal{J} and \mathcal{L} . However, we can reconstruct non-geodesic inequalities at the trajectory level. Given the positivity of $j[\rho_\gamma(t)]$, $\ell^2[\rho_\gamma(t)]$, and $\delta[\rho_\gamma(t)]$, we have the following bound

$$\delta[\rho_\gamma(t)] \leq \frac{4j[\rho_\gamma(t)]}{t^2}. \quad (28)$$

Consequently, we can establish the trajectory-level inequality

$$\frac{\mathcal{I}[\rho_\gamma(t)]}{\delta[\rho_\gamma(t)]} \geq 1, \quad (29)$$

where $\mathcal{I}[\rho_\gamma(t)] = \frac{1}{t} \int_0^t d\tau f_Q[\rho_\gamma(\tau)]$ is the time-averaged CQFI along the trajectory γ (defined for $0 \leq \tau \leq t$).

Previous works [25, 34, 39] have shown that the SLD operator connects the time-derivative of the density matrix to the QFI via the bound

$$\int_0^t dt' \frac{|\dot{\rho}(t')|}{\Delta_{\rho_t} O} \leq \int_0^t dt' \sqrt{f_Q(t')} = 2\mathcal{L}(t). \quad (30)$$

Here, $|\dot{\rho}(t)| = |\text{Tr}[O\dot{\rho}_t]|$ represents the rate of change of the observable expectation value, and $\Delta_{\rho_t} O = \sqrt{\text{Tr}[\rho_t O^2] - \text{Tr}[\rho_t O]^2}$ is the instantaneous variance of the observable O .

We propose analogous bounds for the instantaneous state of a single trajectory, $\rho_\gamma(t) = |\psi_\gamma(t)\rangle\langle\psi_\gamma(t)|$. We define the stochastic rate of change of the observable

as $\dot{\rho}_\gamma(t) = \text{Tr}[O\dot{\rho}_\gamma(t)]$ and the stochastic variance with respect to the instantaneous pure state as $\Delta_{\rho_\gamma(t)} O$. The new single-trajectory speed limit is derived as

$$|\dot{\rho}_\gamma(t)| \leq \Delta_{\rho_\gamma(t)} O \sqrt{f_Q[\rho_\gamma(t)]}. \quad (31)$$

The integral version of this bound yields

$$\int_0^t dt' \frac{|\dot{\rho}_\gamma(t')|}{\Delta_{\rho_\gamma(t')} O} \leq \int_0^t dt' \sqrt{f_Q[\rho_\gamma(t')]} = 2\mathcal{L}[\rho_\gamma(t)]. \quad (32)$$

This inequality represents a fundamental speed limit at the trajectory level. To validate these bounds, we apply them to the jump unraveling of a driven two-level system in contact with a thermal reservoir.

Example: Driven two-level system in a thermal environment

We test these results using a single two-level system coupled to a thermal environment at finite temperature T . The system Hamiltonian is $H_S = \omega\sigma_z$, subject to a time-dependent driving potential $V(t) = \varepsilon(e^{-i\omega t}\sigma_+ + e^{i\omega t}\sigma_-)$, where $\varepsilon \ll \omega$ is the driving amplitude and $\{\sigma_z, \sigma_+, \sigma_-\}$ are the Pauli matrices. The control parameter is defined by the phase factor $\lambda(t) = e^{i\omega t}$.

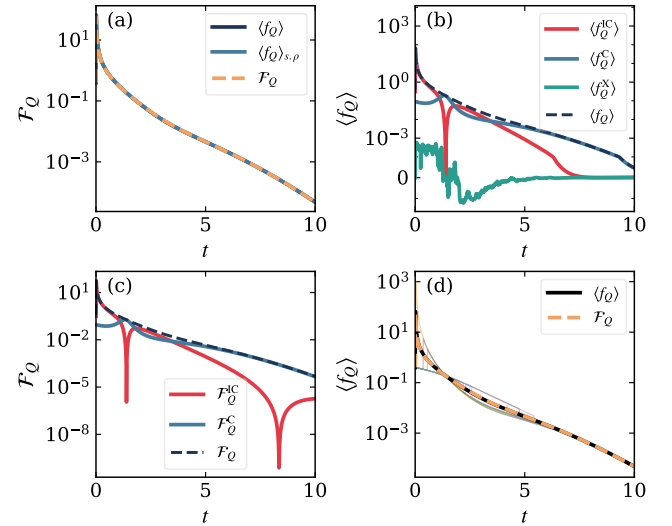


FIG. 2. Decomposition and validation of the CQFI. (a) The agreement of the average CQFI $\langle f_Q \rangle$ (in blue) with the QFI \mathcal{F}_Q (in orange dashed), with relative error $\leq 1\%$. (b) Decomposition of $\langle f_Q \rangle$ into populations $\langle f_Q^C \rangle$, coherent $\langle f_Q^C \rangle$, and cross $\langle f_Q^X \rangle$ contributions. The coherence term dominates at longer times, highlighting the quantum nature of the dynamics. (c) Decomposition of \mathcal{F}_Q (black dashed) into populations \mathcal{F}_Q^C (in red) and coherences \mathcal{F}_Q^C (in blue) contributions, where the cross term is strictly zero. (d) Trajectory level fluctuations of the CQFI (thin lines) compared against the ensemble averages $\langle f_Q \rangle$ (in black) and \mathcal{F}_Q (in orange, dashed).

We assume a cyclic protocol Λ with duration τ , such that $\lambda(0) = \lambda(\tau)$. In the rotating wave approximation, the Hamiltonian becomes $\hat{H}_{RWA} = \varepsilon \hat{\sigma}_x$. As such, the Hamiltonian is time-independent in this frame.

The dynamics are described by the GKSL master equation with jump operators corresponding to the emission and absorption of photons

$$L_- = \sqrt{\Gamma_0(\bar{n}+1)}\sigma_-; \quad L_+ = \sqrt{\Gamma_0\bar{n}}\sigma_+, \quad (33)$$

where Γ_0 is the spontaneous emission rate and $\bar{n} = (e^{\hbar\omega/k_B T} - 1)^{-1}$ is the mean number of thermal photons. For a continuously monitored system, the stochastic Schrödinger equation is given by

$$\begin{aligned} d|\psi_\gamma(t)\rangle = dt \left[-iH_{\text{eff}}(t) + \frac{\Gamma_0}{2}(\langle\sigma_+\sigma_-\rangle - \langle\sigma_-\sigma_+\rangle) \right] |\psi_\gamma(t)\rangle \\ + dN_- \left(\frac{\sigma_-}{\sqrt{\langle\sigma_+\sigma_-\rangle}} - 1 \right) |\psi_\gamma(t)\rangle \\ + dN_+ \left(\frac{\sigma_+}{\sqrt{\langle\sigma_-\sigma_+\rangle}} - 1 \right) |\psi_\gamma(t)\rangle, \end{aligned} \quad (34)$$

where H_{eff} includes the driving and non-Hermitian damping terms. The Poissonian increments dN_\pm take the value 1 when a jump $k = \pm$ occurs and 0 otherwise.

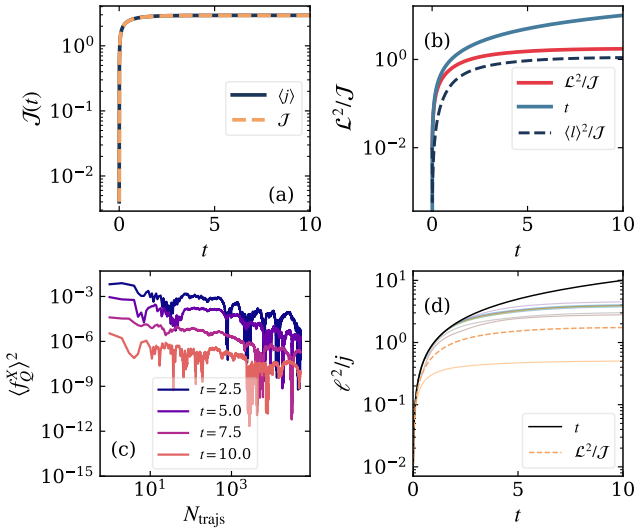


FIG. 3. Verification of information geometry and speed limits. (a) Convergence of the average stochastic action $\langle j \rangle(t)$ to the ensemble-level statistical action $J(t)$. (b) Comparison of speed limits at ensemble and averaged-trajectory level. The bound derived for ensemble QFI is consistently higher than or equal to average of single-trajectories bounds, respecting the expected hierarchy. (c) Convergence of $\langle f_Q^X \rangle$ toward zero as the number of trajectories increases, for different time steps. (d) Verification of the trajectory-level speed limit inequality $l^2 \leq j$ for a subset of the $N_{\text{trajs}} = 5 \times 10^4$ simulated trajectories.

We proceed by calculating the stochastic length $\ell_\Lambda(\gamma_{[0,\tau]})$ for each trajectory. Given the probability

overlap with the ensemble $c_n(\gamma(t)) = \langle n(t)|\psi_\gamma(t)\rangle$, the conditional quantum Fisher information for this two-level system takes the specific form

$$f_Q^{\text{IC}}(\gamma(t)) = \sum_{n=0,1} |c_n(\gamma(t))|^2 \left(\frac{\dot{p}_n(t)}{p_n(t)} \right)^2, \quad (35)$$

$$f_Q^{\text{C}}(\gamma(t)) = \sum_{k=0,1} \left| c_n(\gamma(t)) \frac{2(p_n - p_k)}{p_n + p_k} \langle k(t)|\dot{n}(t)\rangle \right|_{n \neq k}^2, \quad (36)$$

$$\begin{aligned} f_Q^X(\gamma(t)) = \sum_{k \neq n} \text{Re} \left[c_k^*(\gamma(t)) c_n(\gamma(t)) \left(\frac{\dot{p}_k(t)}{p_k} + \frac{\dot{p}_n(t)}{p_n} \right) \right. \\ \times \left. \left(\frac{2(p_n - p_k)}{p_n + p_k} \right) \langle k|\dot{n}(t)\rangle \right]. \end{aligned} \quad (37)$$

The incoherent and coherent terms f_Q^{IC} , and f_Q^{C} are diagonal with relation to the projections on state $|\psi_\gamma(t)\rangle\langle\psi_\gamma(t)|$, and the cross term f_Q^X contains the off-diagonal projections.

The numerical simulations validate our framework, demonstrating that the average CQFI converges to the standard QFI with negligible error, as seen in Fig. 2(a). However, the power of the trajectory-level approach becomes apparent in the spectral decomposition [Fig. 2(b)-(c)]. Unlike the ensemble QFI, the single-trajectory CQFI reveals a significant cross-term f_Q^X arising from the interference between population changes and basis rotations. As illustrated in Fig. 2(d), this term often exhibits negative fluctuations during transient evolution, signaling a destructive interplay between classical and quantum information channels that is strictly non-classical and unobservable in standard ensemble averages.

The numerical results confirm the rigorous consistency of our stochastic information geometry (Fig. 3). We find that the trajectory-averaged action recovers the standard ensemble statistical action, while the speed limits respect the thermodynamic hierarchy: the ensemble-level bound restricts the dynamics more tightly than the average of the stochastic bounds. This statistical convergence is further evidenced by the asymptotic vanishing of the interference cross-term $\langle f_Q^X \rangle$ as the sample size increases. Most importantly, Fig. 3(d) validates that the fundamental geometric uncertainty relation $l^2 \leq j$ is strictly satisfied for every individual realization, establishing the CQFI as a robust metric for single-shot thermodynamic bounds.

To test the speed limits of observables, introduced in Eqs. (30) and (32), we use $\hat{O} = \hat{H}_{\text{RWA}}$, meaning that the speed limit for observables is either $\mathcal{L}(t) \geq 0$ or $\ell(\gamma, t) \geq 0$. The results are depicted in Fig. 4, where 4(a) shows the inequality for the ensemble level, and 4(b) shows for trajectory level, depicting some of the trajectories.

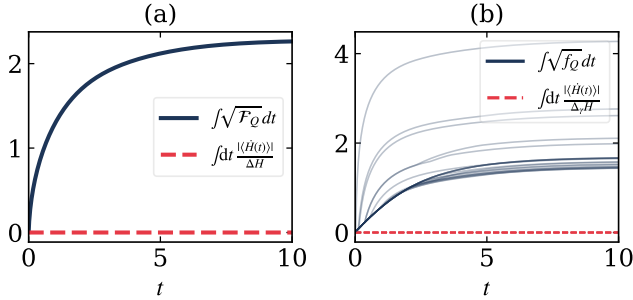


FIG. 4. Speed limits for the rate of change of the Hamiltonian expectation value. (a) Ensemble-level speed limit [cf. Eq.(30)]. (b) Trajectory-level speed limit [cf. Eq.(32)]. Since the Hamiltonian is time-independent in the rotating frame, the rate of change is zero for all times. Consequently, the speed limit inequalities are trivially satisfied, with the geometric bounds (RHS) remaining strictly positive and bounding the zero velocity (LHS) throughout the evolution.

V. CONCLUSIONS AND OUTLOOKS

We established a formal connection between stochastic thermodynamics and quantum information geometry, extending the study of metrological sensitivity from ensemble averages individual quantum trajectories. By introducing the CQFI, we provide a framework that captures the stochastic fluctuations of information flow inherent to continuous quantum measurements.

A key piece of insight from our analysis is the spectral decomposition of the trajectory-level information. We have shown that the sensitivity of a single trajectory is driven by three distinct mechanisms: an incoherent contribution from population shifts, a coherent contribution from basis rotations, and a transient cross-term arising from their interference. Crucially, this term can be negative, a purely quantum phenomenon signifying destructive interference between classical probability updates and unitary evolution. Such negative interference acts as a strictly local witness of non-classicality, as it vanishes exactly in the ensemble average, and provides a new metric for characterizing the quality of state preparation and evolution in quantum estimation tasks.

Building on this geometric structure, we have derived fundamental quantum speed limits valid for single realizations. By defining thermodynamic length and action for individual trajectories, we have demonstrated that the speed of quantum evolution is bounded not just on average, but stochastically for every run of the experiment. These trajectory-level bounds offer a robust thermodynamic interpretation of the CQFI, connecting information-theoretic quantities to the fluctuating energetics of small quantum systems.

Looking forward, our framework opens several promising avenues for quantum control and thermodynamics. First, the decomposition of the CQFI

offers a blueprint for real-time adaptive metrology [40]. By monitoring the stochastic evolution of incoherent and coherent contributions, feedback protocols could dynamically switch measurement bases to exploit transient spikes in sensitivity [41]. Second, the ability of the cross-term to witness destructive interference suggests its usefulness in characterizing efficiency losses in microscopic heat engines or identifying quantum advantages in battery charging protocols at the single-shot level. Finally, the CQFI serves as a natural estimator for importance sampling, allowing for the efficient simulation and identification of rare, high-information trajectories that are typically inaccessible to standard Monte Carlo methods. These tools collectively advance our ability to analyze and optimize quantum dynamics beyond the limitations of ensemble descriptions.

ACKNOWLEDGMENTS

PBM is grateful for discussions with Anna Sanpera, Alessandro Candeloro, Carmem Gilardoni, Diogo Soares-Pinto, Gabriel Bié Alves, Guilherme Zambon, Ivan Medina, and Luis Garcia-Pintos. PBM acknowledges the support of the Brazilian agency Coordenação de Aperfeiçoamento de Pessoal de Ensino Superior (CAPES), finance code 001. PVP acknowledges the Fundação de Amparo à Pesquisa do Estado do Rio de Janeiro (FAPERJ Process SEI-260003/000174/2024). F.I. acknowledges financial support from the Brazilian funding agencies CAPES, CNPQ, FAPERJ (No. 151064/2022-9, and No. E-26/201.365/2022), and by the Serrapilheira Institute (grant number Serra – 2211-42166). SMDQ acknowledges CNPq grant No. 302348/2022-0, and FAPERJ grant No. APQ1-210.310/2024. MP acknowledges support from the Royal Society Wolfson Fellowship (RSWF/R3/183013), the Department for the Economy of Northern Ireland under the US-Ireland R&D Partnership Programme, the PNRR PE Italian National Quantum Science and Technology Institute (PE0000023), and the EU Horizon Europe EIC Pathfinder project QuCoM (GA no. 10032223). WAMM acknowledges CNPq grant No. 308560/2022-1.

Appendix A: Derivation of the Conditional Quantum Fisher Information (CQFI)

For an unknown parameter θ , the classical Stochastic Fisher Information (SFI) associated with a single measurement outcome x is given by

$$\iota(\theta, x) = \left(\frac{\partial \log p(x|\theta)}{\partial \theta} \right)^2. \quad (\text{A1})$$

In the quantum setting, the conditional probability is determined by the Born rule, $p(x|\theta) = \text{Tr}(\Pi_x \rho_\theta)$, where

$\{\Pi_x\}$ constitutes an arbitrary POVM. Recall that the standard Quantum Fisher Information (QFI) is defined as the maximum of the classical Fisher information over all possible POVM measurements

$$\mathcal{F}_Q(\theta) = \text{Tr}(\rho_\theta L_\theta^2) = \max_{\{\Pi_x\}} \mathcal{I}(\theta), \quad (\text{A2})$$

where L_θ is the Symmetric Logarithmic Derivative (SLD) operator satisfying the Lyapunov equation $\partial_\theta \rho_\theta = \frac{1}{2}\{L_\theta, \rho_\theta\}$.

To define the quantum analog of the SFI, denoted as the Conditional Quantum Fisher Information (CQFI). We analyze the kernel of the classical average. Expanding the derivative of the logarithm yields

$$\iota(\theta, x) = \left(\frac{1}{p(x|\theta)} \frac{\partial p(x|\theta)}{\partial \theta} \right)^2 = \left(\frac{\text{Tr}(\Pi_x \partial_\theta \rho_\theta)}{\text{Tr}(\Pi_x \rho_\theta)} \right)^2. \quad (\text{A3})$$

Substituting the SLD identity $\partial_\theta \rho_\theta = \frac{1}{2}\{L_\theta, \rho_\theta\}$ and utilizing the cyclic property of the trace (assuming Π_x is a projector or commutes appropriately), we apply the Cauchy-Schwarz inequality $|\text{Tr}(A^\dagger B)|^2 \leq \text{Tr}(A^\dagger A) \text{Tr}(B^\dagger B)$. By choosing $A = \sqrt{\rho_\theta} \sqrt{\Pi_x}$ and $B = \sqrt{\rho_\theta} L_\theta \sqrt{\Pi_x}$, we obtain the bound

$$\begin{aligned} \iota(\theta, x) &\leq \frac{|\text{Tr}(\Pi_x L_\theta \rho_\theta)|^2}{(\text{Tr}(\rho_\theta \Pi_x))^2} \leq \frac{\text{Tr}(\Pi_x L_\theta^2 \rho_\theta) \text{Tr}(\rho_\theta \Pi_x)}{(\text{Tr}(\rho_\theta \Pi_x))^2} \\ &= \frac{\text{Tr}(\Pi_x L_\theta^2 \rho_\theta)}{\text{Tr}(\rho_\theta \Pi_x)}. \end{aligned} \quad (\text{A4})$$

The quantity on the right-hand side of Eq. (A4) saturates the local information bound and serves as our definition for the CQFI

$$f_{Q,x}(\theta) = \frac{\text{Tr}(\Pi_x L_\theta^2 \rho_\theta)}{\text{Tr}(\rho_\theta \Pi_x)}. \quad (\text{A5})$$

Differently from the standard QFI, which is a global scalar obtained by averaging over all outcomes, the CQFI is a random variable associated with the specific outcome x of a single realization.

Averaging $f_Q(\theta; \Pi_x)$ over the probability distribution of outcomes naturally recovers the QFI

$$\begin{aligned} \langle f_Q \rangle &= \sum_x p(x|\theta) f_{Q,x}(\theta) \\ &= \sum_x \text{Tr}(\Pi_x L_\theta^2 \rho_\theta) \\ &= \text{Tr} \left[\left(\sum_x \Pi_x \right) L_\theta^2 \rho_\theta \right] = \mathcal{F}_Q(\theta), \end{aligned} \quad (\text{A6})$$

where we have utilized the completeness relation $\sum_x \Pi_x = \mathbb{I}$.

Alternatively, we may propose a simpler, state-conditioned formulation for the CQFI

$$f_{Q,\alpha}(\theta) = \text{Tr}(\Pi_\alpha L_\theta^2) = \langle \alpha | L_\theta^2 | \alpha \rangle, \quad (\text{A7})$$

where $\Pi_\alpha = |\alpha\rangle\langle\alpha|$ projects onto an arbitrary state $|\alpha\rangle$. This form quantifies the local sensitivity of the system conditioned on a specific direction in Hilbert space. Unlike the global QFI, estimating this quantity does not require full quantum state tomography to reconstruct the spectrum of ρ_θ .

Appendix B: Spectral Decomposition of the CQFI

To elucidate the physical mechanisms contributing to the CQFI, we assume the density matrix possesses the spectral decomposition $\rho_\theta = \sum_n p_n(\theta) |n_\theta\rangle\langle n_\theta|$. In this eigenbasis, the SLD operator can be expanded as

$$L_\theta = \sum_n \frac{\partial_\theta p_n}{p_n} |n_\theta\rangle\langle n_\theta| + 2 \sum_{n \neq k} \frac{p_n - p_k}{p_n + p_k} \langle n_\theta | \partial_\theta k_\theta \rangle |n_\theta\rangle\langle k_\theta|. \quad (\text{B1})$$

We can decompose the SLD into a diagonal (incoherent) component L_{IC} and an off-diagonal (coherent) component L_C , such that $L_\theta = L_{IC} + L_C$. The squared operator is then given by $L_\theta^2 = L_{IC}^2 + L_C^2 + \{L_{IC}, L_C\}$.

When evaluating the state-conditioned CQFI $f_{Q,\alpha}(\theta) = \langle \alpha | L_\theta^2 | \alpha \rangle$, we must account for the cross-terms between the diagonal and off-diagonal parts. While these cross-terms vanish in the global ensemble average (the trace), they are generally non-zero for a specific state $|\alpha\rangle$. Thus, the CQFI splits into three distinct contributions

$$f_{Q,\alpha}(\theta) = f_{Q,\alpha}^{IC}(\theta) + f_{Q,\alpha}^C(\theta) + f_{Q,\alpha}^X(\theta). \quad (\text{B2})$$

The first term, the incoherent CQFI, is analogous to the classical SFI. It captures the sensitivity arising from changes in the state's eigenvalues

$$f_{Q,\alpha}^{IC}(\theta) = \sum_n |\langle n | \alpha \rangle|^2 \left(\frac{\partial_\theta p_n}{p_n} \right)^2. \quad (\text{B3})$$

The second term, the coherent CQFI f_Q^C , captures the information arising from the unitary rotation of the eigenbasis. This contribution reflects the fact that the eigenstates depend on θ and generally do not commute with their derivatives

$$f_{Q,\alpha}^C(\theta) = \sum_k \left| \sum_{n(\neq k)} \langle n | \alpha \rangle \frac{2(p_n - p_k)}{p_n + p_k} \langle k | \partial_\theta n \rangle \right|^2. \quad (\text{B4})$$

The third term, the cross-term CQFI f_Q^X , represents the interference between the population dynamics and the basis rotations

$$f_{Q,\alpha}^X(\theta) = \sum_{k \neq n} \text{Re} \left[c_k^* c_n \left(\frac{\partial_\theta p_k}{p_k} + \frac{\partial_\theta p_n}{p_n} \right) \right] \quad (\text{B5})$$

$$\times \left(\frac{2(p_n - p_k)}{p_n + p_k} \right) \langle k | \partial_\theta n \rangle, \quad (\text{B6})$$

where $c_n = \langle n|\alpha \rangle$. This term quantifies the correlation between the classical and quantum channels of information. Notably, unlike the incoherent and coherent contributions which are strictly non-negative, the cross-term f_Q^X can be negative. A negative value indicates destructive interference, where the population shifts and geometric rotations partially cancel each other out relative to the probe state $|\alpha\rangle$.

Appendix C: Examples for CQFI

In order to put in place the formal framework illustrated above and attest to the potential of CQFI, we examine two paradigmatic examples: field-sensing with a qubit prepared in a thermal state, and force-sensing through displaced Gaussian states. We demonstrate that the CQFI behaves qualitatively similarly to the QFI, and in specific Gaussian regimes, they coincide quantitatively.

1. Field sensing with a thermal qubit

We consider a two-level system used to estimate a transverse field parameter θ . The system Hamiltonian is $\hat{H}_S(\theta) = \Delta\sigma_z + \frac{\theta}{2}\sigma_x$, where Δ is the energy gap and θ is the transverse driving field. The system is in a thermal state $\rho_\theta = e^{-\beta\hat{H}_S(\theta)}/\mathcal{Z}(\theta)$, where $\mathcal{Z}(\theta) = \text{Tr}(e^{-\beta\hat{H}_S(\theta)})$.

The eigenvalues of the Hamiltonian are $E_\pm(\theta) = \pm\frac{\Omega(\theta)}{2}$, with the generalized Rabi frequency $\Omega(\theta) = \sqrt{\Delta^2 + \theta^2}$. The equilibrium populations are

$$p_\pm(\theta) = \frac{1}{2} \left[1 \mp \tanh \left(\frac{\beta\Omega(\theta)}{2} \right) \right]. \quad (\text{C1})$$

The incoherent contribution to the CQFI, arising from the population derivatives, is

$$f_{Q,\Pi_\pm}^{\text{IC}}(\Pi_\pm, \theta) = \frac{\beta^2\theta^2}{4\Omega^2(\theta)} \left[1 \pm \tanh \left(\frac{\beta\Omega(\theta)}{2} \right) \right]^2. \quad (\text{C2})$$

The coherent contribution, arising from the misalignment between the field and the quantization axis, is given by

$$f_{Q,\Pi_\pm}^{\text{C}}(\theta) = \frac{\Delta^2}{\Omega^4(\theta)} \tanh \left(\frac{\beta\Omega(\theta)}{2} \right). \quad (\text{C3})$$

Note that f_Q^{C} vanishes only if $\beta = 0$ (infinite temperature) or $\Delta = 0$ (no gap). The total CQFI is the sum of these two terms. This example illustrates how the CQFI allows us to distinguish between information gained from thermal population shifts versus information gained from the rotation of the energy eigenbasis.

2. Force sensing in dislocated Gaussian states

Dislocated Gaussian states are a prominent resource in quantum metrology, particularly for weak force

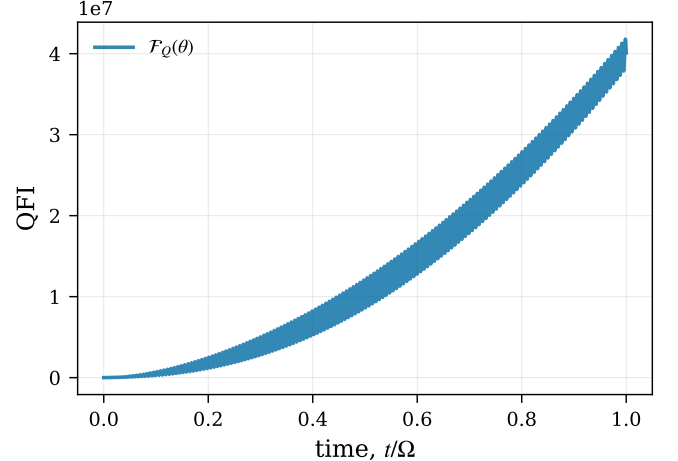


FIG. 5. Time evolution of the CQFI and QFI for force sensing in dislocated Gaussian states. Due to the Gaussian nature of the state and measurement, the CQFI coincides with the QFI. Both quantities scale quadratically with time, $\mathcal{F}_Q \sim t^2$.

estimation. We consider a harmonic oscillator under a constant force θ , described by the Hamiltonian $\hat{H} = \hbar\omega\hat{a}^\dagger\hat{a} - \theta\hat{x}$.

Gaussian systems are fully characterized by their first and second moments. The optimal SLD operator for estimating the displacement parameter θ is given by [42, 43]

$$\hat{L}_\theta = \frac{2t}{\det(V)} [V_{xp}(\hat{x} - \langle \hat{x} \rangle) - V_x(\hat{p} - \langle \hat{p} \rangle)], \quad (\text{C4})$$

where V is the covariance matrix. The resulting QFI is

$$\mathcal{F}_Q(\theta) = \text{Tr}(\rho\hat{L}_\theta^2) = \frac{4t^2V_x}{\det(V)}. \quad (\text{C5})$$

To compare this bound with a trajectory-level quantity, we consider a continuous weak measurement of the position quadrature, described by Gaussian POVM elements

$$\hat{\Pi}_x(\alpha) = \left(\frac{4k\Delta t}{\pi} \right)^{1/4} \exp(-2k\Delta t(\hat{x} - \alpha)^2), \quad (\text{C6})$$

where α is the measurement outcome. The CQFI for this measurement is defined as

$$f_{Q,\alpha}(\theta) = \frac{\text{Tr}(\rho\hat{\Pi}_x(\alpha)\hat{L}_\theta^2)}{\text{Tr}(\rho\hat{\Pi}_x(\alpha))}. \quad (\text{C7})$$

Remarkably, solving the Gaussian integrals reveals that

$$f_{Q,\alpha}(\theta) = \frac{4t^2V_x}{\det(V)} = \mathcal{F}_Q(\theta). \quad (\text{C8})$$

The CQFI is independent of the stochastic measurement outcome α . This is a consequence of the Gaussian

statistics: while the measurement outcome α shifts the center of the Wigner function (updating the first moments), the curvature (second moments) and the sensitivity to the displacement force remain invariant.

Thus, in this specific Gaussian regime, the single-trajectory information is identical to the ensemble average.

[1] M. G. A. Paris, Quantum estimation for quantum technology, *International Journal of Quantum Information* **07**, 125 (2009), <https://doi.org/10.1142/S0219749909004839>.

[2] G. Tóth and I. Apellaniz, Quantum metrology from a quantum information science perspective, *Journal of Physics A: Mathematical and Theoretical* **47**, 424006 (2014).

[3] J. Liu, H. Yuan, X.-M. Lu, and X. Wang, Quantum fisher information matrix and multiparameter estimation, *Journal of Physics A: Mathematical and Theoretical* **53**, 023001 (2019).

[4] V. Montenegro, C. Mukhopadhyay, R. Yousefjani, S. Sarkar, U. Mishra, M. G. Paris, and A. Bayat, Quantum metrology and sensing with many-body systems, *Physics Reports* **1134**, 1 (2025).

[5] N. F. Ramsey, A molecular beam resonance method with separated oscillating fields, *Phys. Rev.* **78**, 695 (1950).

[6] D. J. Wineland, J. J. Bollinger, W. M. Itano, F. L. Moore, and D. J. Heinzen, Spin squeezing and reduced quantum noise in spectroscopy, *Phys. Rev. A* **46**, R6797 (1992).

[7] V. Giovannetti, S. Lloyd, and L. Maccone, Advances in quantum metrology, *Nature Photon.* **5**, 222 (2011).

[8] L. Pezzè, A. Smerzi, M. K. Oberthaler, R. Schmied, and P. Treutlein, Quantum metrology with nonclassical states of atomic ensembles, *Rev. Mod. Phys.* **90**, 035005 (2018).

[9] G. M. D'Ariano, M. D. Laurentis, M. G. A. Paris, A. Porzio, and S. Solimeno, Quantum tomography as a tool for the characterization of optical devices, *Journal of Optics B: Quantum and Semiclassical Optics* **4**, S127 (2002).

[10] M. G. Genoni, S. Olivares, and M. G. A. Paris, Optical phase estimation in the presence of phase diffusion, *Phys. Rev. Lett.* **106**, 153603 (2011).

[11] R. Demkowicz-Dobrzański, J. Kolodyński, and M. Guta, The elusive Heisenberg limit in quantum-enhanced metrology, *Nature Commun.* **3**, 1063 (2012).

[12] I. Frerot and T. Roscilde, Quantum critical metrology, *Phys. Rev. Lett.* **121**, 020402 (2018).

[13] L. Garbe, M. Bina, A. Keller, M. G. A. Paris, and S. Felicetti, Critical quantum metrology with a finite-component quantum phase transition, *Phys. Rev. Lett.* **124**, 120504 (2020).

[14] Y. Chu, S. Zhang, B. Yu, and J. Cai, Dynamic framework for criticality-enhanced quantum sensing, *Phys. Rev. Lett.* **126**, 010502 (2021).

[15] M. M. Taddei, B. M. Escher, L. Davidovich, and R. L. de Matos Filho, Quantum speed limit for physical processes, *Phys. Rev. Lett.* **110**, 050402 (2013).

[16] A. del Campo, I. L. Egusquiza, M. B. Plenio, and S. F. Huelga, Quantum speed limits in open system dynamics, *Phys. Rev. Lett.* **110**, 050403 (2013).

[17] S. Deffner and E. Lutz, Quantum speed limit for non-markovian dynamics, *Phys. Rev. Lett.* **111**, 010402 (2013).

[18] G. E. Crooks, Measuring thermodynamic length, *Phys. Rev. Lett.* **99**, 100602 (2007).

[19] E. H. Feng and G. E. Crooks, Far-from-equilibrium measurements of thermodynamic length, *Phys. Rev. E* **79**, 012104 (2009).

[20] D. A. Sivak and G. E. Crooks, Thermodynamic metrics and optimal paths, *Phys. Rev. Lett.* **108**, 190602 (2012).

[21] S. Ito, Stochastic thermodynamic interpretation of information geometry, *Phys. Rev. Lett.* **121**, 030605 (2018).

[22] S. B. Nicholson, A. del Campo, and J. R. Green, Nonequilibrium uncertainty principle from information geometry, *Phys. Rev. E* **98**, 032106 (2018).

[23] S. Ito and A. Dechant, Stochastic time evolution, information geometry, and the cramér-rao bound, *Phys. Rev. X* **10**, 021056 (2020).

[24] S. B. Nicholson, L. P. García-Pintos, A. del Campo, and J. R. Green, Time-information uncertainty relations in thermodynamics, *Nature Physics* **16**, 1211 (2020).

[25] L. P. García-Pintos, S. B. Nicholson, J. R. Green, A. del Campo, and A. V. Gorshkov, Unifying quantum and classical speed limits on observables, *Phys. Rev. X* **12**, 011038 (2022).

[26] P. B. Melo, F. Iemini, D. O. Soares-Pinto, S. M. D. Queirós, and W. A. M. Morgado, Thermodynamic interpretation to stochastic fisher information and single-trajectory speed limits, *Phys. Rev. E* **112**, 014126 (2025).

[27] H. Touchette, The large deviation approach to statistical mechanics, *Phys. Rep.* **478**, 1 (2009).

[28] J. P. Garrahan, Aspects of non-equilibrium in classical and quantum systems: Slow relaxation and glasses, dynamical large deviations, quantum non-ergodicity, and open quantum dynamics, *Physica A* **504**, 130 (2018).

[29] H. M. Wiseman and G. J. Milburn, *Quantum Measurement and Control* (Cambridge University Press, Cambridge, 2009).

[30] K. Jacobs, *Quantum Measurement Theory and its Applications* (Cambridge University Press, Cambridge, 2014).

[31] P. B. Melo, S. M. Duarte Queirós, and W. A. M. Morgado, Stochastic thermodynamics of fisher information, *Phys. Rev. E* **111**, 014101 (2025).

[32] G. Tóth and D. Petz, Extremal properties of the variance and the quantum fisher information, *Phys. Rev. A* **87**, 032324 (2013).

[33] S. Campbell, I. D'Amico, M. A. Ciampini, J. Anders, N. Ares, S. Artini, A. Auffèves, L. B. Oftelie, L. P. Bettmann, M. V. Bonança, T. Busch, M. Campisi, M. F. Cavalcante, L. A. Correa, E. Cuestas, C. B. Dag, S. Dago, S. Deffner, A. del Campo, A. Deutschmann-Olek, S. Donadi, E. Doucet, C. Elouard, K. Ensslin, P. Erker, N. Fabbri, F. Fedele, G. Fiusa, T. Fogarty, J. A. Folk, G. Guarneri, A. S. Hegde, S. Hernández-Gómez, C.-K. Hu, F. Iemini, B. Karimi, N. Kiesel, G. Landi, A. Lasek, S. Lemziakov, G. Lo Monaco, E. Lutz, D. Lvov,

O. Maillet, M. Mehboudi, T. M. Mendonça, H. J. D. Miller, A. K. Mitchell, M. Mitchison, V. Mukherjee, M. Paternostro, J. P. Pekola, M. Perarnau-Llobet, U. G. Poschinger, A. Rolandi, D. Rosa, R. Sánchez, A. C. Santos, R. S. Sarthour, E. Sela, A. Solfanelli, A. M. Souza, J. Splettstoesser, D. Tan, L. Tesser, T. V. Vu, A. Widera, N. Yunger Halpern, and K. Zawadzki, Roadmap on quantum thermodynamics, *Quantum Science and Technology* (2025).

[34] L. P. Bettmann and J. Goold, Information geometry approach to quantum stochastic thermodynamics, *Phys. Rev. E* **111**, 014133 (2025).

[35] G. Manzano and R. Zambrini, Quantum thermodynamics under continuous monitoring: A general framework, *AVS Quantum Science* **4**, 025302 (2022).

[36] J. M. Horowitz and J. M. R. Parrondo, Entropy production along nonequilibrium quantum jump trajectories, *New Journal of Physics* **15**, 085028 (2013).

[37] C. Elouard, D. A. Herrera-Martí, M. Clusel, and A. Auffèves, The role of quantum measurement in stochastic thermodynamics, *npj Quantum Information* **3**, 9 (2017).

[38] D. P. Pires, M. Cianciaruso, L. C. Céleri, G. Adesso, and D. O. Soares-Pinto, Generalized geometric quantum speed limits, *Phys. Rev. X* **6**, 021031 (2016).

[39] J. Bringewatt, Z. Steffen, M. A. Ritter, A. Ehrenberg, H. Wang, B. S. Palmer, A. J. Kollár, A. V. Gorshkov, and L. P. García-Pintos, Generalized geometric speed limits for quantum observables (2024), arXiv:2409.04544 [quant-ph].

[40] H. M. Wiseman, Adaptive phase measurements of optical modes: Going beyond the marginal q distribution, *Phys. Rev. Lett.* **75**, 4587 (1995).

[41] F. Albarelli, M. A. C. Rossi, D. Tamascelli, and M. G. Genoni, Restoring Heisenberg scaling in noisy quantum metrology by monitoring the environment, *Quantum* **2**, 110 (2018).

[42] A. Monras, Phase space formalism for quantum estimation of gaussian states (2013), arXiv:1303.3682 [quant-ph].

[43] S. Chang, M. G. Genoni, and F. Albarelli, Multiparameter quantum estimation with gaussian states: efficiently evaluating holevo, rld and sld cramér-rao bounds (2025), arXiv:2504.17873 [quant-ph].